



ELSEVIER

Journal of Magnetism and Magnetic Materials 172 (1997) 69–73

M Journal of
M magnetism
M and
magnetic
materials

New technique to measure magnetic anisotropy using the vectorial magneto-optic Kerr effect

S.M. Jordan^{a,*}, C. Prados^b

^a *Research Institute for Materials, University of Nijmegen, Toernooiveld 1, NL-6525 ED Nijmegen, The Netherlands*

^b *Instituto de Magnetismo Aplicado, Universidad Complutense – RENFE, Madrid, Spain*

Received 4 February 1997; received in revised form 11 April 1997

Abstract

A new method of interpreting the data produced by vectorial magnetometry using the magneto-optic Kerr effect (MOKE) is described. The procedure allows the angle between the magnetisation and the applied field to be measured independently of the applied field. Rotation of the sample generates a curve similar to that produced by a torque magnetometer. The technique is applied to sputtered Si/Co/Cr/Co trilayers, and the curves are analysed using a fitting method to measure the ratio of the magnetisation to the uniaxial anisotropy constant, providing an insight into the effects of thermal annealing on the samples.

PACS: 75.70; 07.55.G; 75.30.G; 75.60.N; 78.20.L

Keywords: MOKE; Torque magnetometry; Magnetic anisotropy; Magnetic multilayers

1. Introduction

In recent years, the magnetic anisotropy displayed by a magnetic sample has commonly been measured by using a torque magnetometer. This instrument has the advantage that it produces data in a compact and meaningful format which easily supports quantitative measurements of anisotropy.

The technique has also been extended to allow measurement of magnetisation [1] and coercivity [2].

This paper outlines a method by which vectorial magneto-optic Kerr effect (MOKE) data can be interpreted to provide data of a comparable quality. The use of MOKE has the advantages of applicability to coverages of only a few atomic layers and in-situ UHV measurement [3]. Data interpretation in this manner eases both quantitative and qualitative measurement of anisotropy and allows comparison with other techniques.

The main difference between the torque magnetometer and this technique is that the former

* Correspondence address: Solid State II, Postbus 9010, 6500 GL Nijmegen, The Netherlands; Tel.: + 31 24 365 2081; fax: + 31 24 365 2190; e-mail: jstr@sci.kun.nl.

only measures one parameter [1], namely the torque produced per unit volume of sample:

$$L = MH \sin \theta, \quad (1)$$

where H is the applied field, M is magnetisation and θ the angle between the two; whereas the vectorial technique measures components of M along two (not necessarily orthogonal) axes. This allows θ to be measured under all conditions, even when $H = 0$.

Experimentally, the sample is rotated (varying α , the angle between the easy axis and H), with hysteresis loops being made at successive angles. The two components of M are measured by changing the incident polarisation which selects different elements in the magneto-optic permittivity tensor [4]. The hysteresis curves are then analysed to yield θ as a function of α for various H .

2. Theory

Following Miyajima [5], the free energy of a uniaxial ferromagnetic film with M in the plane of the film can be written as the sum of an anisotropic and a magnetostatic energy:

$$E_{\text{total}} = -K \cos^2(\theta - \alpha) - MH \cos \theta, \quad (2)$$

with K in erg/cc, M in emu/cc and H in Oe. The angles θ and α are as defined above. The total energy will have a minimum at the point

$$\frac{d}{d\theta}(E_{\text{total}}) = K \sin 2(\theta - \alpha) + MH \sin \theta = 0, \quad (3)$$

provided that the second derivative is positive. An approximate solution to a similar equation in the general case was obtained by Wielinga [1]; however, for the purposes of this paper it is sufficient to identify two cases: those of large field (small θ), and zero field. When the ratio MH/K is large, the approximation

$$\theta \approx \frac{\sin 2\alpha}{2 \cos 2\alpha + MH/K} \quad (4)$$

is valid. This gives the familiar high-field torque curve, which becomes more and more sinusoidal as H increases.

Under the conditions of low field, the equation

$$\sin(\alpha - \theta) = 0, \quad (5)$$

is valid, and is satisfied by $\theta = \alpha + n\pi$. The magnetisation processes are such that $-\pi/2 < \theta < \pi/2$, resulting in a sawtooth shape with respect to α .

The Kerr rotation displayed by the sample for the two incident polarisations used, 5 and 45°, can be written as

$$\sigma^5 = M_{\text{sat}}(V_l^5 \cos \theta + V_t^5 \sin \theta), \quad (6)$$

$$\sigma^{45} = M_{\text{sat}}(V_l^{45} \cos \theta + V_t^{45} \sin \theta). \quad (7)$$

The V values relate the magnetisation referred to M_{sat} to the voltage seen at the detector [6]. The subscripts l and t refer to field in the longitudinal and transverse directions, respectively, and the superscripts to the incident polarisation. Magnetic field is applied along the longitudinal direction ($\theta = 0$). From the two measurements (Eqs. (6) and (7)), we deduce that θ can be found using

$$\tan \theta = \frac{\sigma^{45} V_l^5 - \sigma^5 V_l^{45}}{\sigma^{45} V_t^5 - \sigma^5 V_t^{45}}, \quad (8)$$

provided that the determinant,

$$\Delta = V_l^5 V_t^5 - V_l^{45} V_t^{45}, \quad (9)$$

is non-zero. The four V parameters are found by experiment.

3. Sample preparation

A Co 200 Å/Cr 40 Å/Co 200 Å trilayer was grown by RF planar magnetron sputtering on water-cooled intrinsic Si(1 1 1). The discharge gas was Ar at a pressure of 5×10^{-3} mbar, the base pressure being 10^{-7} mbar. The deposition rates were 0.8 and 0.9 Å s⁻¹ for the Co and Cr, respectively. The sample was then cut into four pieces, three of them being annealed at nominal temperatures of 200, 300 and 400°C. The samples were then held at the specified temperature for 1 h, the time for both heating and cooling being approximately 15 min. It was believed that these samples would show sensitivity to thermal annealing due to the possibility of

interdiffusion between the layers. The annealing behaviour of the samples is also of interest since this type of structure has been the subject of further study [7].

4. Moke measurements

The MOKE measurements were made using an instrument described elsewhere [6]. In each case, the field changed at a rate of 0.01 Hz. The samples were rotated with a field of 100 Oe applied to ensure that each loop was reversible and not due to a 'virgin' state. The values of the four constants in Eq. (8) were found by applying a field sufficient to cause saturation (300 Oe) to the samples along both the longitudinal and transverse directions and measuring the resulting magneto-optic rotation. The ratio of V_t to V_l (transverse to longitudinal sensitivity) as a function of incident polarisation is shown in Fig. 1. These values compare favourably with those calculated from bulk values at an angle of incidence of 82° using equations given by Florczak and Dahlberg [8]. We explain the observed

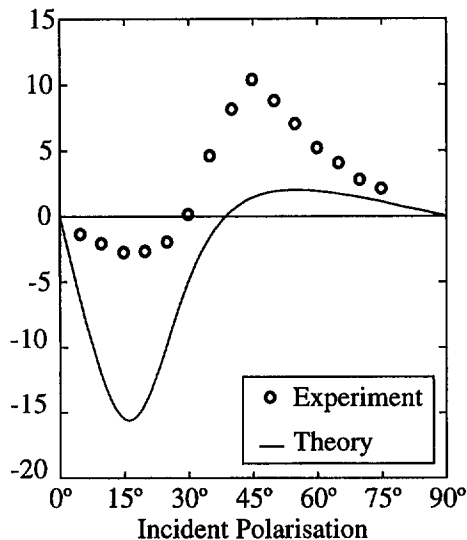


Fig. 1. The ratio of V_t to V_l as a function of incident polarisation angle. The x-axis is defined as the angle between the p -plane and the E vector. The line shows the calculation made from bulk values for Co described in Section 4.

discrepancy by the fact that the films differ from bulk in that light reflected from the interface beneath a 200 Å film plays an important part in both the reflectivity and magneto-optic rotation of the film [9].

The hysteresis curves for both polarisations were analysed by measuring the differences in signal at various points as shown in Fig. 2. Measurements within the closed portion of the loop were not made other than at the remanent points. The coercivities of the films were all approximately 12 Oe.

The data were then analysed to resolve the angle of magnetisation, θ , using Eq. (8), care being taken to obtain the correct sign. The values of θ were then fitted manually to curves obtained by numerical solution of a modified form of Eq. (3):

$$\sin 2(\theta - \alpha) + \gamma \sin \theta = 0, \quad (10)$$

with the condition that the second derivative of the energy was positive. Here,

$$\gamma \equiv \frac{MH}{K}, \quad (11)$$

and is a measure of the shape of the 'torque' (θ versus α) curve. High values of γ indicate high field (or low anisotropy), with the shape more sinusoidal. Typical curves are shown in Fig. 3. The relation between γ , as determined from the fitting process, and the value of the applied field was fitted to the law

$$\gamma = gH + c, \quad (12)$$

with the gradient, g , being equal to M/K .

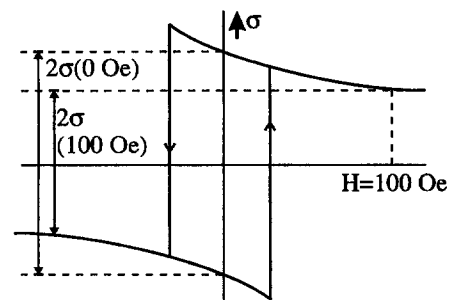


Fig. 2. Illustration of the way in which σ was measured. The line $\sigma = 0$ cannot be used since the loop has an arbitrary offset.

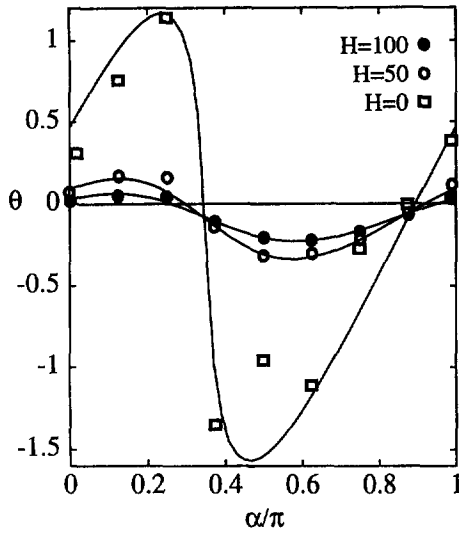


Fig. 3. Comparison between experimental and fitted data for three different applied fields. Note the offset which appears in the data. Sample annealed to 300°C.

5. Results and discussions

The relations between γ and H are shown in Fig. 4. It is immediately clear that the parameter c (Eq. (12)) is non-zero in three cases. This means that the curve does not change to the sawtooth as described in Section 2, but remains curved as though a small field were applied. We attribute this fact to the polycrystallinity of the films, some regions of the film have slightly different easy directions. All the films were found to have uniaxial anisotropy.

The phenomenon of a film grown on an ordered substrate displaying a uniaxial anisotropy has been reported by Baird et al. [10] for the case of Co/Si (1 1 1) and Durand et al. [11] for Fe/MgO (1 0 0). The latter case was found to be due to in-plane tetragonal distortion of the Fe film caused by the oblique angle of incidence during deposition. The case of Co/Si is less well-understood – Baird et al. found a uniaxial anisotropy in a Co film of thickness 125 Å deposited on an oxidised Si wafer. Using a fitting procedure (which assumed coherent rotation) to analyse the complete loops, they found values of K/M to be about 18 Oe. Various origins

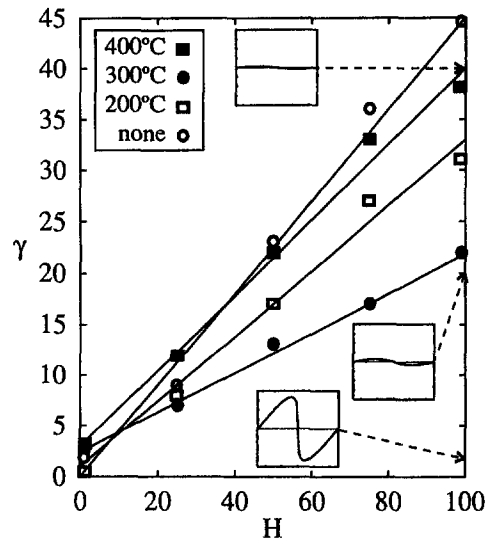


Fig. 4. Relation between the values of γ found from the fitting process and the applied field for the four samples. Lines of best fit are also shown – a larger gradient corresponds to a smaller K . The inset graphs show the corresponding θ versus α curves for three different values of γ .

for this effect were proposed although no direct evidence was found. The isolation of a particular cause (such as strain or defects within the substrates) is not possible without further insight.

It is clear that the torque curves are not centered exactly along the line $\theta = 0$, but a small offset is present, especially at zero field. This is perhaps due to the presence of a stray field. During the data analysis, it was found that the average of σ^{45} over the whole range of α at high field was not constant between the samples. This may indicate that the saturation magnetisation (see Eq. (7)) decreased significantly as the anneal temperature increased, provided that the optical properties of the samples remained constant. Both the values of σ^5 , and those of σ^{45} taken at low fields, did not show such a consistent decrease, the reason for this being unclear. A similar effect of the applied field was observed – increasing the applied field increased the mean value of σ^{45} by up to 20%, indicating that the assumption of constant M is not strictly valid.

Table 1 summarises both the anisotropy and the average value of σ^{45} data. Since the link between

Table 1

Summary of data from the samples. The value of K/M is obtained from the gradient of the γ versus H graph, and K absolute uses the bulk value of M for Co.

Anneal temp.	σ^{45} mean (relative)	K/M (Oe)	K absolute (erg/cc)
None	100	2.27	3.2×10^3
200	80	3.12	4.4×10^3
300	72	5.13	7.2×10^3
400	53	2.71	3.8×10^3

the average signal and saturation magnetisation is not proven, we have used the bulk magnetisation value of Co to calculate illustrative values of K . It was clear that annealing to 300°C increased the anisotropy, higher temperatures causing a subsequent reduction of K .

Acknowledgements

This research was supported by the Engineering and Physical Sciences Research Council (EPSRC), and by the European Union under contract number CHRX-CT930320.

References

- [1] T. Wielinga, *J. Appl. Phys.* 50 (1979) 4888.
- [2] J. Hur, S.-C. Shin, *Appl. Phys. Lett.* 62 (1993) 2140.
- [3] S. Bader, J. Erskine, in: B. Heinrich, J. Bland (Eds.), *Ultra-thin Magnetic Structures*, vol. II, ch. 4, Springer, Berlin 1994, p. 297.
- [4] R. Hunt, *J. Appl. Phys.* 38 (1967) 1652.
- [5] H. Miyajima, K. Sato, T. Mizoguchi, *J. Appl. Phys.* 47 (1976) 4669.
- [6] S. Jordan, *J. Whiting*, *Rev. Sci. Instrum.* 67 (1996) 4286.
- [7] H. Niedoba et al., *Phys. Status Solidi (a)* 158 (1996) 259.
- [8] J. Florczak, E.D. Dahlberg, *J. Appl. Phys.* 67 (1990) 7520.
- [9] E. Moog, S. Bader, J. Zak, *Appl. Phys.* 56 (1990) 2687.
- [10] M. Baird et al., *J. Appl. Phys.* 74 (1993) 5658.
- [11] O. Durand et al., *J. Magn. Magn. Mater.* 145 (1995) 111.